JACS
JOURNAL OF THE AMERICAN CHEMICAL SOCIETY

Article

pubs.acs.org/JACS

Photo-Controllable DNA Origami Nanostructures Assembling into Predesigned Multiorientational Patterns

Yangyang Yang,[†] Masayuki Endo,*[,‡,§] Kumi Hidaka,[†] and Hiroshi Sugiyama*[,†,‡,§]

[†]Department of Chemistry, Graduate School of Science, Kyoto University, Kitashirakawa-oiwakecho, Sakyo-ku, Kyoto 606-8502, Japan

[‡]Institute for Integrated Cell-Material Sciences (WPI-iCeMS), Kyoto University, Yoshida-ushinomiyacho, Sakyo-ku, Kyoto 606-8501, Japan

[§]CREST, Japan Science and Technology Corporation (JST), Sanbancho, Chiyoda-ku, Tokyo 102-0075, Japan

Supporting Information

ABSTRACT: We demonstrate a novel strategy for constructing multidirectional programmed 2D DNA nanostructures in various unique patterns by introducing photoresponsive oligonucleotides (Azo-ODNs) into hexagonal DNA origami structures. We examined regulation of assembly and disassembly of DNA nanostructures reversibly by different photoirradiation conditions in a programmed manner. Azo-ODNs were incorporated to the hexagonal DNA origami structures, which were then employed as self-assembly units for building up nanosized architectures in regulated arrangements. By adjusting the numbers and the positions of Azo-ODNs in the hexagonal units, the specific nanostructures with face controlling can be achieved, resulting in construction of ring-shaped nanostructures. By combining DNA origami strategy with photoregulating system, remote controlling of assembly and disassembly of DNA nanostructures has been accomplished simply by photo irradiation.

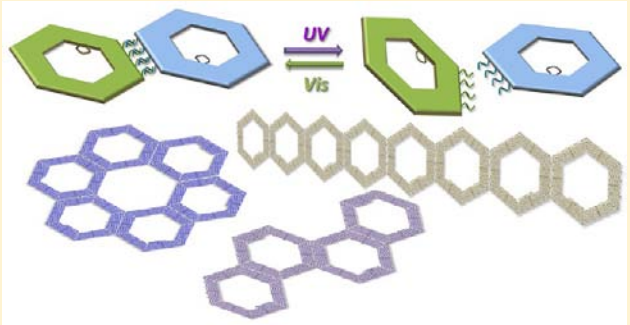

INTRODUCTION

Because of the defined double-helical structure and highly specific base pairing system, DNA has been explored as versatile building blocks for a variety of nanosized architectures. In the past few decades, DNA nanotechnology has already achieved great progress, especially the emergence of DNA origami technology.[1] On the basis of the DNA origami method, various multidimensional nanoarchitectures including the two-dimensional (2D) and three-dimensional (3D) structures even with the curved geometries were successfully developed with predesigned size and shape. Moreover, the following functionalizations for various applications have emerged and blossomed.[2,3] Because of spatial addressability in nanospace and extremely excellent biocompatibility, DNA nanostructures have already been applied to the organization of heteroelements such as proteins,[4−6] nanoparticles,[7−9] and synthetic molecules[10,11] and employed as nanoscaffolds for single-molecule analysis.[2] However, directional controlling and structural diversity are still the challenges. There have already a few strategies for programmed DNA origami assembly published for constructing various architectures in supersize or in a multiple patterns.[12−14] Yan and co-workers developed a strategy referred to as "superorigami" to scale up individual origami tiles into larger spatially addressable nanostructures.[15] The origami tiles could be directed onto a loose framework preprepared from a single-stranded DNA with bridge strands. Our group have already developed "Jig-saw pieces" strategy and realized the construction 1D and 2D programmed nanostructures.[16−18]

Here, we demonstrate another distinctive photoregulated self-assembly method for organizing defined regular or irregular DNA architectures composed of photoresponsive DNA origami units by introducing azobenzene-modified oligonucleotides (Azo-ODNs). The assembly and disassembly between each origami unit should be regulated by photoinduced isomerization of azobenzene moieties in wavelength-dependent manner.[19−21] We recently directly observed the hybridization and dissociation of photoresponsive oligonucleotides in the DNA nanostructure.[22] This shows that a pair of photoresponsive oligonucleotides containing azobenzene moieties can effectively work as an adhesive switch even at the single-molecule level.

The design of the single DNA origami unit in hexagonal shape with around 55 nm outer edge and 33 nm inner edge is shown in Figure 1a. The staples located on the outer edges are connected to Azo-ODNs by disulfide bond (Supporting Information). Two pseudocomplementary photoresponsive short oligonucleotides, Azo-ODN 1 and Azo-ODN 2, containing different numbers of *trans*-form azobenzene

Received: August 6, 2012
Published: December 4, 2012

   dx.doi.org/10.1021/ja307785r | J. Am. Chem. Soc. 2012, 134, 20645−20653

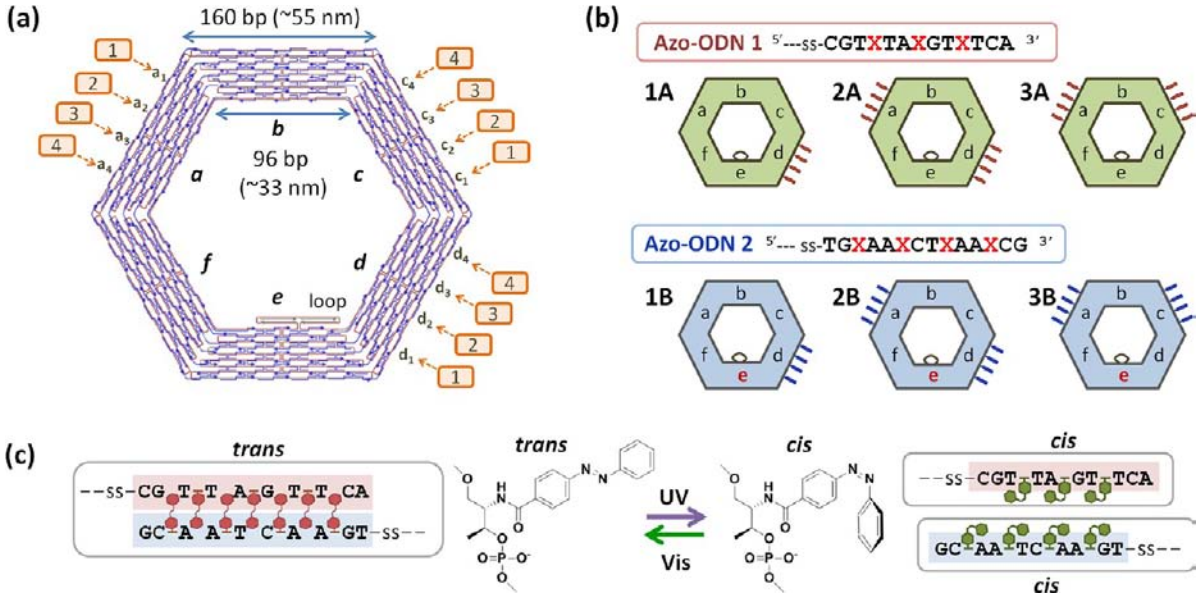

Figure 1. Schematic drawings of photoresponsive DNA origami structure. (a) Design of hexagonal shaped unit where each of three edges (a, c, d) was used for introduction of four azobenzene-modified oligonucleotides (Azo-ODN) in counterclockwise order. (b) Sequences of the two pseudocomplementary Azo-ODNs used in this study and scheme for different modified patterns of hexagonal unit, green hexagons (A-series) are modified with four Azo-ODN 1 strands and blue ones (B-series) are modified with four Azo-ODN 2 strands. For identification of hexagonal monomers, hairpin DNA markers were introduced to the e-domain of the B-series monomers (marked by red colored "e"). (c) Hybridization and dissociation of Azo-ODN 1 and Azo-ODN 2 controlled by *trans*−*cis* photoisomerization of azobenzene moiety under UV and visible light (Vis) irradiation.

moieties were introduced to DNA origami structures.[19−22] These Azo-ODNs form duplex in *trans*-form under visible light irradiation and dissociate in *cis*-form under UV-irradiation by reversible *trans*−*cis* photoisomerization (Figure 1b,c). Since conventional rectangular DNA origami whose edges cause interactions with other origami, here all of the six edges of the hexagonal shaped origami unit are in the direction of helical axis avoiding the π-stacking interactions with others.[1,16] Three edges (a-, c-, and d-) of A- and B-series of hexagonal origami units were chosen for the modification with Azo-ODN 1 and Azo-ODN 2, respectively. Four Azo-ODNs were introduced to the edges at the position labeled with a_1, a_2, a_3, a_4, and so forth, in counterclockwise order (Figure 1a). The A-series hexagonal units were modified by Azo-ODN 1 containing three azobenzene molecules (dark red bars), while the B-series were with Azo-ODN 2 containing four azobenzene molecules (blue bars). Each series had three types of modification: "d-edge" (**1A** and **1B**), "a-/d-edges" (**2A** and **2B**), and "a-/c-edges" (**3A** and **3B**) (Figure 1b). By adjusting the number and the position of Azo-ODN-modified staples, the photo-responsive hexagonal origami units assembling into prede-signed oligomeric nanostructures could be precisely controlled. We also intended to build up a series of photoregulated DNA origami supernanostructures in both linear and curved arrangement.

RESULTS AND DISCUSSION

Hexagonal Monomer and Dimer. A long single-stranded DNA, M13mp18, with the help of custom-designed staple strands was folded into a hexagonal shaped structure. In the atomic force microscope (AFM) image of hexagonal origami, a loop was clearly observed at the inner side of e-domain marked with orange triangle (Figure 2a). In the expanded images, we observed that the hexagonal monomers were monodisperse

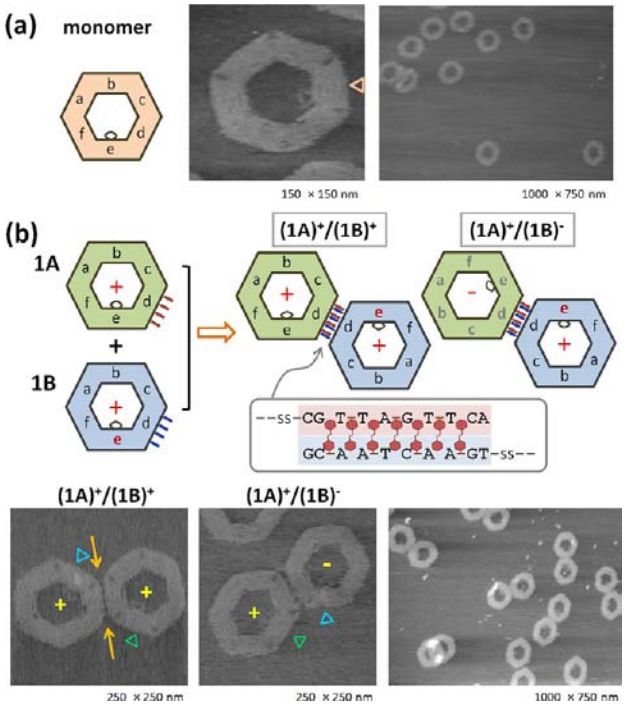

Figure 2. Hexagonal monomer and dimer formation via photo-responsive ODNs. (a) Schematic drawing of unmodified monomer and AFM images after annealing. The loop of e-domain was marked by orange triangle. (b) Two different monomers (**1A**-unit and **1B**-unit) were employed for self-assembly of dimer. Hairpin markers were introduced into **1A** unit to distinguish two different monomers, and the facing orientaions of two monomers could be differentiated by the relative position of loops at e-domain of **1A** and **1B**. Two orange arrows indicated the four hybridized Azo-ODN duplexes between d-edges of **1A** and **1B**.

dx.doi.org/10.1021/ja307785r | J. Am. Chem. Soc. 2012, 134, 20645−20653

without aggregation. These hexagonally shaped units were then employed as components for the construction of photoregulated supernanostructures with the help of Azo-ODN duplexes.

We first tried the construction of hexagonal dimer using four-Azo-ODN-modified hexagonal unit at d-edge, in which one unit (**1A**) and another one (**1B**) were modified with Azo-ODN 1 strands and Azo-ODN 2 strands, respectively. After the preparation of two monomers carrying pseudocomplementary Azo-ODNs separately, we carried out the assembly of dimers by mixing two Azo-ODN-modified monomers together at an annealing rate of −0.1 °C/min from 50 to 15 °C. Under the visible light, the azobenzene molecules maintained the *trans*-form facilitating the hybridization of Azo-ODN 1 and Azo-ODN 2, and subsequently the dimer could be formed. Both of the hexagonal origami units were symmetrical, so that two types of hexagonal dimer should be obtained (Figure 2b) because the connection between the two units lacks relative facing up/down control. One type of the dimer would be in the same facing orientation ("+/+") while another type would be in the relatively opposite orientation ("+/−"). In the AFM images, relative orientation of hexagonal units could be distinguished by the positions of the loop at the inner side of e-domain (Figure 2b, marked with blue and green triangles). In addition, hairpin markers were introduced to the center of e-domain in the B-series hexagonal units to differentiate two monomers. Four short photoresponsive connecting duplexes pointed by two orange arrows were clearly observed between the hexagons, which represented that the two monomers were connected together by photoresponsive ODNs, indicating that the hexagonal units were not just absorbed at the close position of the mica surface in coincidence. In the expanded AFM image shown here, the dimer self-assembly worked with high yield over 90%.

Evaluation of Reversible Assembly and Disassembly of Hexagonal Oligomers. As already mentioned above, the photoresponsive ODNs introduced as connection arms here were employed not only for the complementarity between Azo-ODN 1 and Azo-ODN 2 but also for the photoinduced reversible hybridization and dehybridization of these two Azo-ODNs. The photoisomerization of azobenzene molecules can regulate the hybridization and dissociation of two short Azo-ODNAs reversibly by UV irradiation (<380 nm) and visible light irradiation (>400 nm).[20] Therefore, we prospected to manually regulate assembly and disassembly of hexagonal oligomers by irradiating between UV and visible light. Here, the hexagonal dimer was employed as a model system for photoirradiation with different wavelength to examine the reversible self-assembly performance (Figure 3a). It was reported that the photoirradiation time and the temperature affects the dissociation and association of Azo-ODN duplex.[20] Initially, it was needed to evaluate the disassembly efficiency of dimers under different temperatures and UV irradiating time to find the optimal conditions. Considering the potential damage of origami structure at relatively high temperature,[23] we first evaluated the effect of temperature on the structure. Agarose gel analysis of hexagonal dimer under different temperatures and UV irradiation time revealed that there was almost no breakage of the individual structures when the temperature was controlled less than 40 °C (Figure S1). In addition, increasing temperature and extending UV irradiation time could both improve the efficiency of the dimer disassembling into the hexagonal monomers. Then, we investigated the reversible

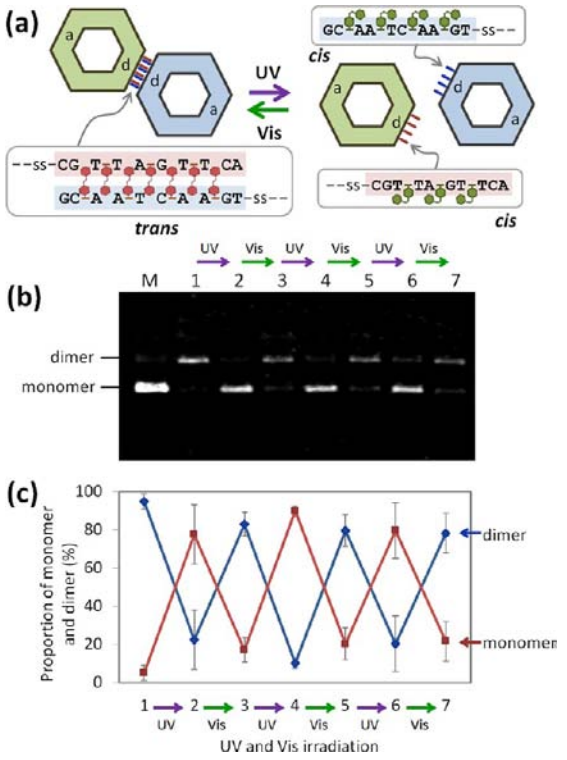

Figure 3. Reversible photoregulation for the formation and dissociation of hexagonal dimer under different irradiation conditions. (a) Schematic drawings of photoregulation of dimers. (b) Agarose gel (0.6%) electrophoresis analysis of the reversible photoregulation for the formation and dissociation between dimer and monomer by UV and visible light (Vis) irradiation. (c) Proportion of dimer and monomer under different irradiation conditions by quantification of the band intensity in (b). Lane M represented the monomer without modification employed as a marker.

photoinduced disassembly and assembly by switching between the UV (350 nm) and visible light irradiation (450 nm) for 5 min at 40 °C. As shown in Figure 3b, by alternating irradiation wavelength by bandpass filters, the hexagonal dimer and monomer can be switched feasibly and reversibly with relatively high yield (from lane 1 to lane 7). After the irradiation of UV light, the dimers were disassembled into monomers because of the dissociation of Azo-ODN duplexes caused by photoisomerization of azobenzene moieties (lane 2). The following irradiation with visible light reassembled the monomers, and the dimers were formed again in a few minutes (lane 3) due to the hybridization of the Azo-ODN strands. In addition, during the consecutive rounds of photoirradiation to the same sample, the assembly and disassembly of the dimers still worked well (from lane 4 to lane 7). Figure 3c shows the proportion of dimer and monomer after three rounds of UV/vis irradiation, and the proportion of the dimer reached 80%, which clearly demonstrates that azobenzene modified oligonucleotides successfully regulate the assembly and disassembly of ∼50 nm-sized DNA nanostructures not only reversibly but repeatedly (another two repeated results were shown in Figure S2). Furthermore, it can be deduced that other programmed patterns of hexagonal oligomers should be also performed in a similar fashion under the different photoirradiation conditions. It is noteworthy that such reversible assembly and disassembly was used for the reconstitution of two pieces repeatedly, and more significantly this photoregulating process can initialize

dx.doi.org/10.1021/ja307785r | J. Am. Chem. Soc. 2012, 134, 20645−20653

and recombine each specific unit in homology, similar to the card shuffling.

Photocontrolled Dynamic Assembly and Disassembly of Hexagonal Units. We next investigated real-time dimer assembly and disassembly by ensemble fluorescence measurement (Figure 4). For **1A**-unit, we introduced 14 nucleotide (nt)

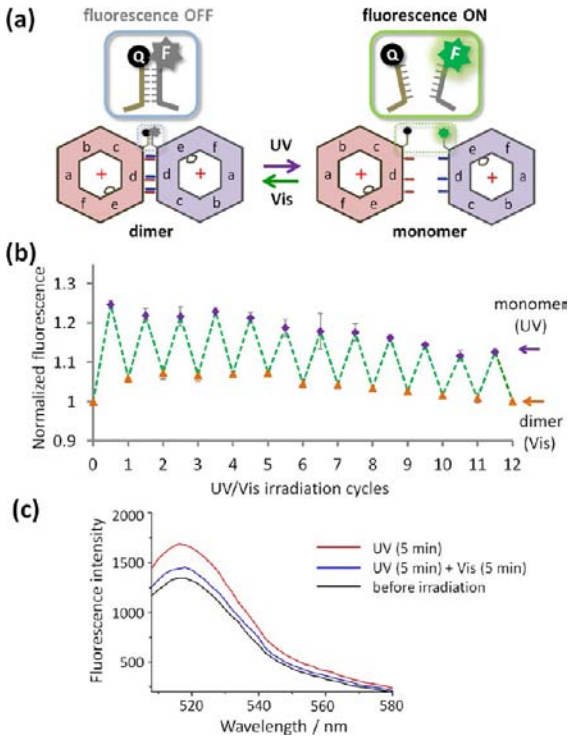

Figure 4. Dynamic dimer formation and dissociation in solution under different irradiation conditions. (a) Schematic of two monomer units labeled by FAM (5′-end) and BHQ1 (3′-end) and fluorescence switching during monomer and dimer formation regulated by UV and visible light irradiation. (b) Reversible fluorescence intensity changes in dimer and monomer states. The numbers of horizontal axis referred to UV/vis irradiation rounds. (c) Fluorescence spectral change of the formation and dissociation of hexagonal dimer. Conditions: excitation, 490 nm; emission recorded, 516 nm; 40 °C.

overhang containing T_8 spacer (eight thymidine) and 6 nt strand carrying BHQ-1 (3′ terminus) as a quenching group to of the c/d corner. Meanwhile, for **1B**-unit, the d/e corner was modified by 14 nt overhang containing T_8 spacer and the complementary 6 nt strand having a FAM group (5′ terminus) as a fluorophore. Fluorescence can be quenched by the formation of dimer with the same facing orientation under visible light irradiation, while it can be turned on in monomer state by UV light (Figure 4a). To increase the quenching efficiency in the dimer state, here three Azo-ODNs in the asymmetrical arrangement (Figure 4a) were introduced into each kind of unit for the formation of dimers in the same facing orientation ("+/+"). As evident in Figure 4b, the real-time fluorescence quenching (λ_{ex}, 490 nm; λ_{em}, 516 nm) can be switched reversibly even over ten rounds of irradiation cycle between UV and visible light. Fluorescence spectral change in one cycle of UV−vis irradiation is also shown in Figure 4c. These results show that the photoinduced dynamic assembly and disassembly of the dimers in solution can be monitored by using the fluorescence quenching system incorporated to the hexagonal monomers.

Hexagonal Trimers in Both Linear and Curved Arrangement without Facing Up/Down Control. Considering the shape of hexagonal origami and the specific hybridization of Azo-ODNs, we tried to build up the extended nanostructures in both linear and curved arrangement. The linear hexagonal trimer was first designed and constructed utilizing **2A** and **1B** hexagonal units. The **2A**-unit carrying Azo-ODN 1 strands in two edges (a- and d-) were assembled with two **1B**-units having Azo ODN 2 strands in d-edge for the linear trimer arrangement. The two kinds of hexagonal units employed here were both symmetrical since the four Azo-ODN strands in the hexagonal structure were distributed uniformly along the edge. We predicted that there would be three types of linear trimers formed without facing up/up control: "(**1B**)−/(**2A**)+/(**1B**)−", "(**1B**)+/(**2A**)−/(**1B**)−", and "(**1B**)+/(**2A**)+/(**1B**)+" (shown in Figure 5). The method for constructing trimer was similar to dimer. After the preparation of two monomers separately, **2A** monomer was mixed with **2B** monomer (2 equiv), and the mixture was annealed from 50 to 15 °C at a rate of −0.05 °C/min. The structures of the trimer were then confirmed by AFM (Figure 4). As expected, three types of trimers with different facing orientations were imaged by AFM in the same reaction solution. In Figure 4a, the two **1B**-units were in the same facing orientations while the middle **2A**-unit was in the opposite. In Figure 4b, one **1B**-unit was the same facing orientation as **2A**-unit while another **1B**-unit was in the opposite facing orientation. In these two types of trimers, one **1B**-unit and one **2A** unit were in mirror symmetry. In Figure 4c, all the units were in the same facing orientation. Here using same self-assembly substrates and annealing conditions, we obtained three types of linear patterns of hexagonal trimers with different facing orientations at the same time. Using agarose gel electrophoresis, the yield of the linear trimers reached around 70% under the above-mentioned annealing conditions (Figure S3).

We next designed and constructed hexagonal trimers in curved arrangement using different self-assembly substrates. We employed **3A** hexagonal unit with a-/c- edge modification with Azo-ODN 1 strands and associate it with **1B**-unit carrying Azo-ODN 2 strands to accomplish the construction of curved trimers using the same annealing conditions of linear trimers. The design and the imaging results were shown together in Figure 6. Because of the same assembling mechanism of the linear trimer formation, three types of trimers in curved arrangement were obtained with the identical permutations and combinations of **3A**-unit and **1B**-unit. The corresponding AFM images in Figure 6 were consistent with the predesigned arrangement. Therefore, the curved trimers in three types were successfully constructed using the same self-assembly substrates without facing up/up control. The yields of the both two kinds of trimers were also confirmed by agarose gel electrophoresis (Figure S3), resulting over 80%. Considering the symmetry of hexagonal units having four Azo-ODN strands along the edges, different types of trimers with multiple facing orientations were prepared from the same self-assembling substrates.

Hexagonal Oligomers without Facing Up/Down Control. For the expansion of the assembled nanostructures, hexagonal oligomers were constructed by using **2A**-unit and **2B**-unit as assembling substrates (Figure 7a). After mixing the two kinds of monomers in the same equivalence, the annealing of self-assembling was first started nonlinearly from 50 to 35 °C by decreasing the temperature by 6 °C at a rate of −0.01 °C/min and increasing it by 3 °C at a rate of +0.5 °C/min and then

dx.doi.org/10.1021/ja307785r | J. Am. Chem. Soc. 2012, 134, 20645−20653

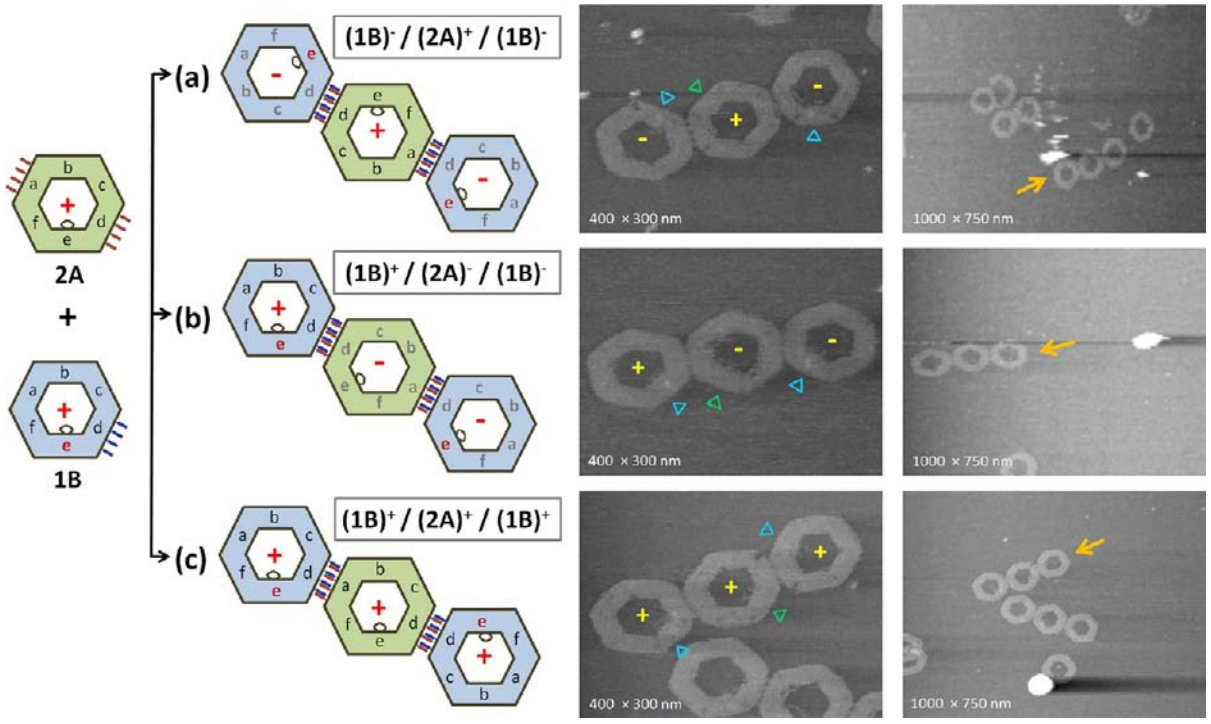

Figure 5. Schematic drawings and AFM images of hexagonal trimers in the linear arrangement using **2A**-unit and **1B**-unit as self-assembly substrates. Three types of trimers were designed and imaged: (a) "(**1B**)−/(**2A**)+/(**1B**)−", (b) "(**1B**)+/(**2A**)−/(**1B**)−", (c) "(**1B**)+/(**2A**)+/(**1B**)+". The three types of trimers could be distinguished by the three individual positions of loops at the e-domain.

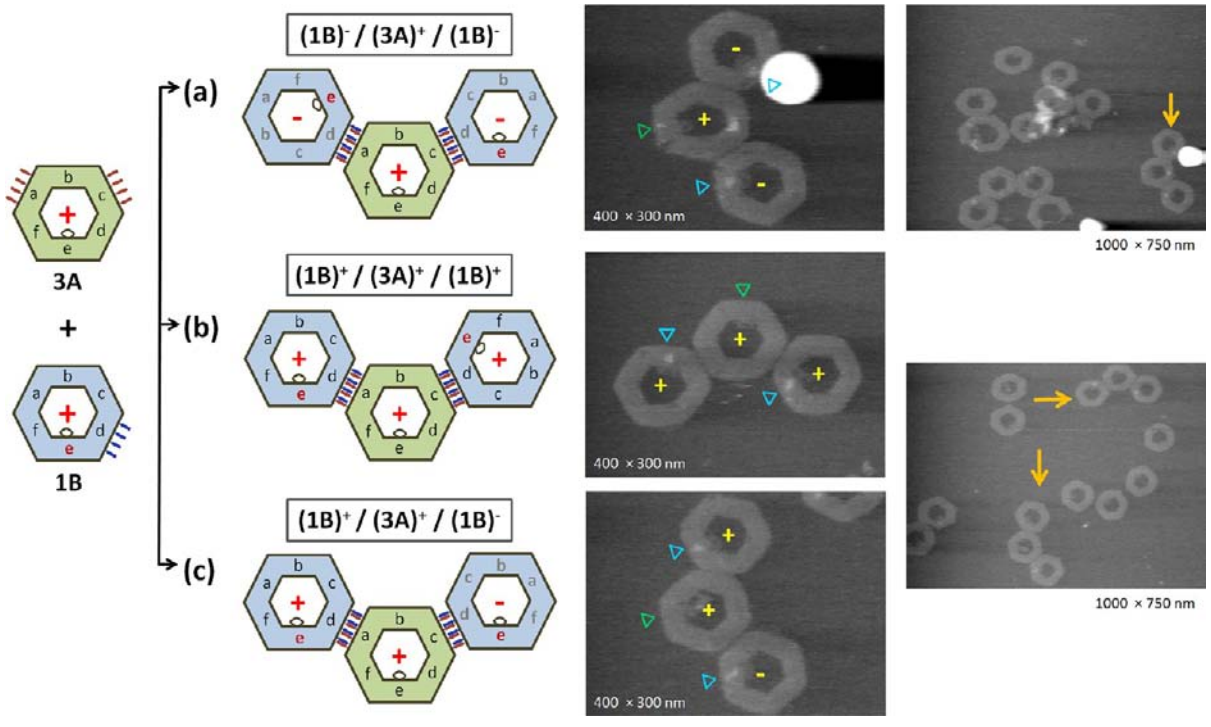

Figure 6. Schematic drawings and AFM images of hexagonal trimers in the curved arrangement using **3A**-unit and **1B**-unit as self-assembly substrates. Three types of trimers were designed and imaged: (a) "(**1B**)−/(**3A**)+/(**1B**)−", (b) "(**1B**)+/(**3A**)+/(**1B**)+", (c) "(**1B**)+/(**3A**)+/(**1B**)−". The three types of trimers could be distinguished by the three relative positions of loops at the e-domain.

gradually decreased from 35 to 15 °C linearly at a rate of −0.01 °C/min. The completed sample was then loaded onto the agarose gel, and retarded oligomer bands appeared in the gel image (lane 1, Figure 7c), indicating that oligomeric structures were formed by assembling of **2A** and **2B** units. The oligomeric structures were observed by AFM (Figures 7d and S4). Here the self-assembling orientations of hexagonal units were still in multiple patterns since each unit had two kinds of assembling orientations, resulting that loops of the hexagonal unit were found as a random arrangement. The longest oligomers imaged

dx.doi.org/10.1021/ja307785r | J. Am. Chem. Soc. 2012, 134, 20645−20653

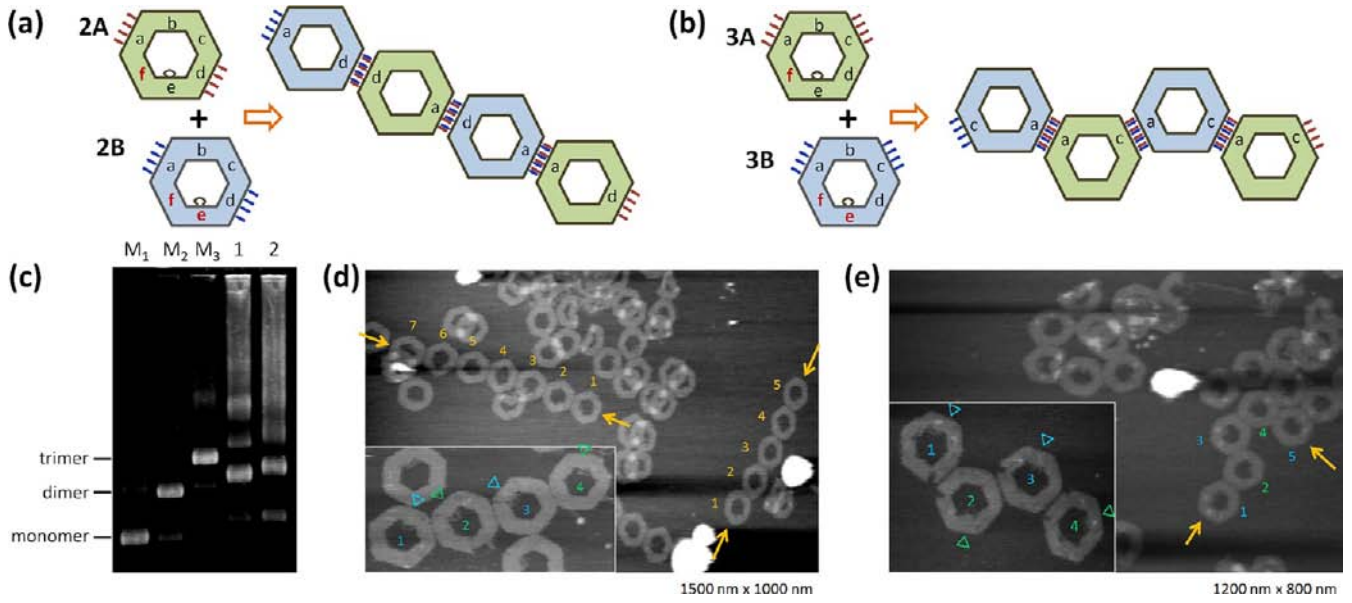

Figure 7. (a) Schematic drawings and AFM images of hexagonal multimers. (a) Assembled oligomers in the linear arrangement using **2A**-unit and **2B**-unit. (b) Assembled oligomers in the curved arrangement using **3A**-unit and **3B**-unit. Hairpin markers were introduced to the f-domain of the A-series monomers and the e-/f-domain of the B-series monomers. (c) Agarose gel (0.4%) image of assemblies from **2A** and **2B** (lane 1) and **3A** and **3B** (lane 2). Lanes M_1, M_2, and M_3 were unmodified monomer, dimer (**1A**−**1B**), and linear trimer (**1B**−**2A**−**1B**), respectively. (d) AFM images of **2A**−**2B** oligomers. Inset: **2A**−**2B** tetramer in linear shape; image size 500 nm × 250 nm. Orange arrows represent assembled oligomers. (e) AFM images of **3A**−**3B** oligomers. Inset: **3A**−**3B** tetramer in zigzag shape; image size 400 nm × 300 nm.

could be obtained as long as seven units. Because of the potential fracture of oligomers when the samples were being loaded on the mica surface, it was speculated that there would be probably much longer nanostructures in the solution as indicated in the gel electrophoresis.

To disassemble the oligomers formed here, we carried out UV irradiation to the sample. After UV irradiation for 5 min, the sample was observed by AFM (Figure S5). Most of the oligomers changed to the monomers (around 90% yield), indicating that the assembled oligomeric structures can be easily reverted to the monomers by UV irradiation.

Meanwhile, we also tried to use **3A**-unit and **3B**-unit as assembling substrates to construct larger curved shaped oligomers (Figure 7b). The same annealing conditions were employed for assembling. After annealing, slower migrated bands appeared in the gel (lane 2, Figure 7c), and the different patterns of oligomers in zigzag shape were imaged by AFM (Figures 7e and S6). In this method, it was basically difficult to control the assembling orientations such as closed ring shape because of the symmetry of adhesive four Azo-ODN connectors in the hexagonal units.

Hexagonal Oligomers in Both Linear and Curved Arrangements with Facing Up/Down Control. We next attempted to design and construct oligomers in only one assembling direction by modifying the numbers of photoresponsive ODNs in the hexagonal units into asymmetrical arrays, as used in the fluorescence labeled dimer in Figure 4. As shown in Figure 8a, each edge was modified with three photoresponsive ODNs at the positions of 1, 2, and 4 in the asymmetrical arrangement in the a-, c-, and d-edges. Six different hexagonal units bearing three Azo-ODN strands at each edge were then prepared (Figure 8b). Hexagonal **5A**-unit and **4B**-unit were employed for the construction of linear trimers and **6A**-unit and **4B**-unit for curved trimers by using the same annealing conditions as trimers with four Azo-ODN connections. As shown in Figure 8c, for the full-matching trimer in the linear arrangement, **5A**-unit and **4B**-unit should be in the opposite orientation for the "(−/+/−)" arrangement. In the AFM image, we only observed the correct arrangement of trimer. For the curved trimer (Figure 8d), **6A**-unit and **4B**-unit can also be well controlled with the facing up/down in the opposite orientation. In both arrangements, the change of symmetry by modifying the number of connecting strands of the hexagonal units can regulate the self-assembled structures into the assigned orientation.

Orientation-Controlled Large Self-Assembled Nanostructures. As already confirmed by trimers with facing control, taking advantage of this strategy, we tried to construct larger sized oligomeric nanostructures in different programmed patterns with facing up/down control. For the extended long linear arrangement of hexagonal oligomers, **5A**-unit and **5B**-unit were employed as self-assembling units. Under the same nonlinear followed by linear annealing conditions as the previous oligomers using four Azo-ODN connectors, the assembled structures were imaged by AFM. As shown in Figure 9a, the linear oligomers containing six units were obtained. For the linear oligomers, the self-assembling orientations could be controlled because of the asymmetry of three Azo-ODN connections between **5A**-units and **5B**-units. However, there were two kinds of assembling modes, "a/a or d/d connection" and "a/d connection", for the linear oligomers, resulting in two kinds of relative positions of the loops at the e-domain (illustrated in Figure 9a, orange dashed box). The alternative facing up/down orientation in the assembled structure should stabilize the whole structure even the three connections of Azo-ODNs were used.

For the curved arrangement to prepare closed ring shape assemblies, the arrangement problem of symmetry can be avoided by using three Azo-ODN connections. After the annealing using **6A**-unit and **6B**-unit as self-assembly substrates,

dx.doi.org/10.1021/ja307785r | J. Am. Chem. Soc. 2012, 134, 20645−20653

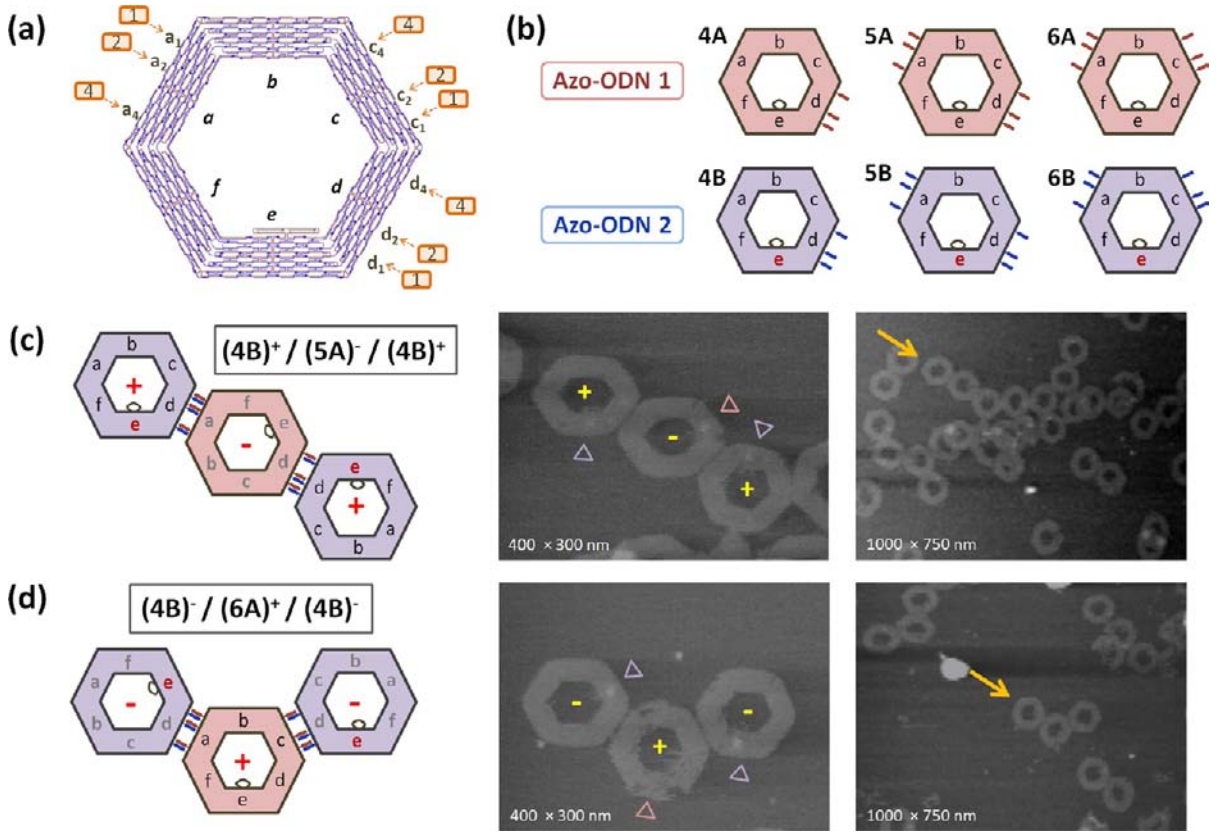

Figure 8. Schematic drawings and AFM images of hexagonal trimers in both linear and curved arrangement with facing up/down control. (a) Design of asymmetrical hexagonal unit by three Azo-ODN strands at the position of 1, 2, and 4 along the edges of hexagonal monomer. (b) Six different patterns of hexagonal monomers were modified with Azo-ODN 1 strands (A-series) and Azo-ODN 2 strands (B-series). For identification of hexagonal monomers, hairpin DNA markers were introduced to the e-domain of the B-series monomers (marked by red colored "e"). (c) Linear trimers with facing up/down control in the arrangement of "(**4B**)+/(**5A**)−/(**4B**)+" were assembled from **4B**-unit and **5A**-unit and imaged by AFM. (d) Curved trimers with facing control in the arrangement of "(**4B**)−/(**6A**)+/(**4B**)−" were assembled from **4B**-unit and **6A**-unit and imaged by AFM. The relative facing orientation of trimers could be distinguished by the three relative positions of the loops at the e-domain.

a ring shaped hexamer was successfully obtained in the arrangement of alternative connection of **6A**-units and **6B**-units (Figure 9b). From the positions of loops of each unit, the neighboring two units were found to be in the relative "+/−" facing orientation as designed. Moreover, other oligomers including ring shaped pentamer and tetramer (Figure S7) and curved shape (Figure S8) were observed with the same alternative arrangement probably because of the elasticity of connecting Azo-ODN duplexes. Above all, hexagonal oligomers in both linear and curved arrangements with facing up/down control could be realized by changing the numbers of Azo-ODN connections in an asymmetrical way along the edges of hexagonal units.

CONCLUSION

We have designed and constructed a series of ∼50 nm-sized hexagonal DNA origami structures, functionalized them with photoresponsive oligonucleotides, and assembled them into various 2D oligomeric nanostructures in both regular and irregular fashions. Considering the hybridization and dissociation of the photoresponsive oligonucleotides associated with the simple photoresponse of azobenzene molecules, the assembly and disassembly of the various DNA nanostructures can be manipulated just by photoirradiation of different wavelengths. By changing the number and the position of the photoresponsive oligonucleotides, the self-assembling orientations can also be controlled more critically. These newly designed photoresponsive DNA nanostructures can be regulated repeatedly between assembly and disassembly states by photoirradiation in a shuffling fashion, which shows great potential for the applications in nanotechnology such as nanomedicine and nanomechanics.

MATERIALS AND METHODS

Materials. All the staple DNAs for the DNA hexagonal unit were purchased from Operon Biotechnology (Tokyo, Japan). Single stranded M13mp18 viral DNA was purchased from New England Biolabs, Inc. The DNA strands for further modification with photoresponsive strands were purchased from Japan Bio Services (Saitama, Japan). The gel-filtration column and the sephacryl S-300 were purchased from BioRad Laboraries (Hercules, CA) and GE Healthcare (Bucking Hamshire, U.K.), respectively. Tris-HCl, EDTA, $MgCl_2$, and agarose for electrophoresis analysis were purchased from Nacalai Tesque, Inc. (Kyoto, Japan). Water was deionized (18.0 MΩ cm specific resistance) by a Milli-Q system (Millipore Corp., Bedford, MA). The hairpin marker sequence used was 5′- TCC TCT TTT GAG GAA CAA GTT TTC TTG T-3′.

Preparation of Hexagonal Units. The hexagonal DNA origami was designed using caDNAno software. The unit was assembled in 20 μL of solution containing 10 nM M13mp18 single stranded DNA, 100 nM staple oligonuclotides (10 equiv), 20 mM Tris buffer (pH 7.6), 1 mM EDTA, and 10 mM $MgCl_2$. The mixture was annealed by reducing the temperature from 85 to 15 °C at a rate of −1.0 °C/min. The origami solution was purified using Sephacryl S-300 gel-filtration

dx.doi.org/10.1021/ja307785r | J. Am. Chem. Soc. 2012, 134, 20645−20653

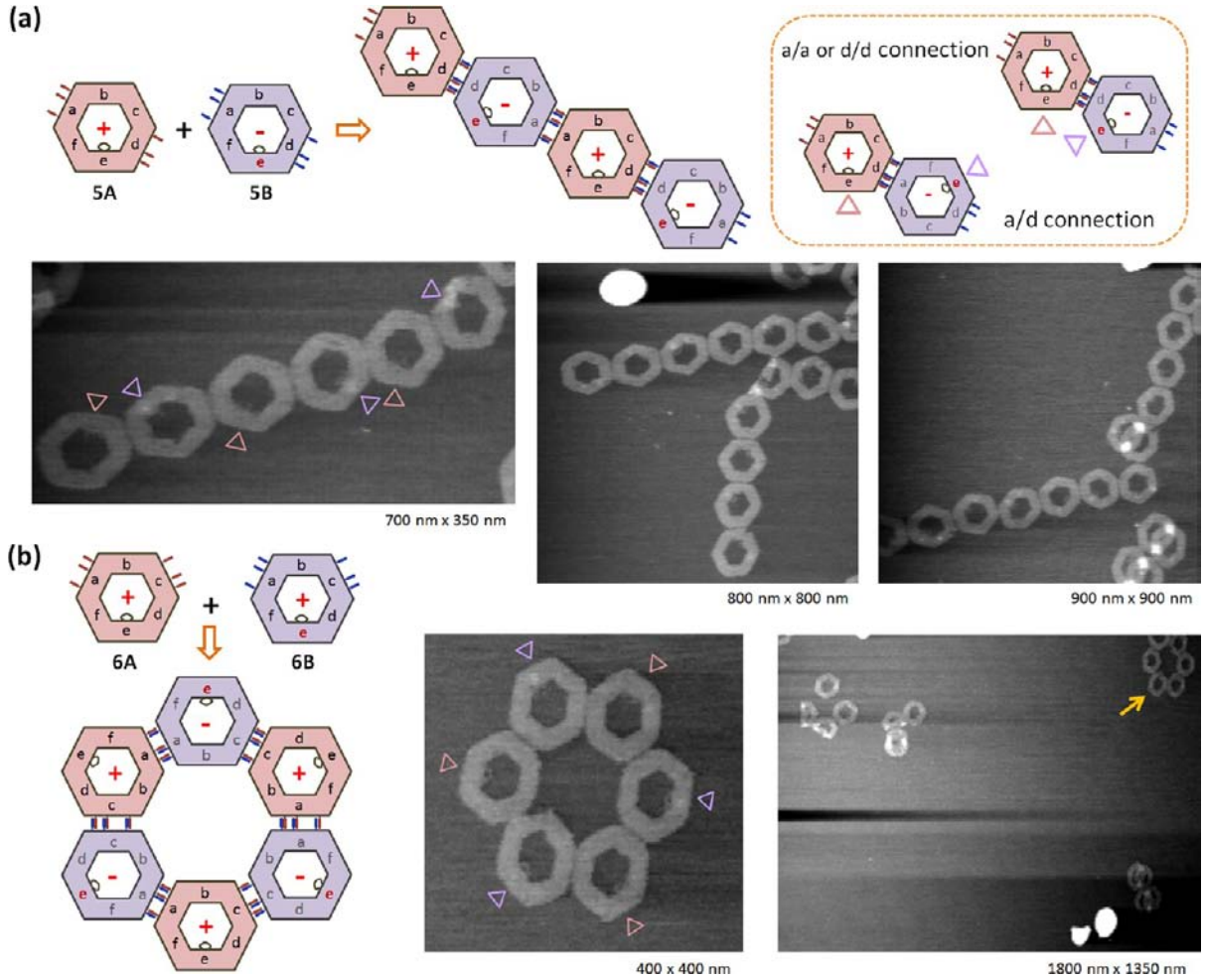

Figure 9. Schematic drawings and AFM images of hexagonal oligomers in the linear (a) and ring arrangement (b) with facing up/down control using the hexagonal units modified with three Azo-ODN strands along each outer-edge. The dashed orange box represented two kinds of assembling modes: "a/a or d/d" and "a/d" connection. The relative facing orientation could be distinguished by the relative positions of loops at the e-domain.

column after annealing finished. The hexagonal units bearing Azo-ODN strands were prepared by replacing the staples modified with Azo ODN strands at the same position according to the design of different patterns of oligomers.

AFM Imaging. AFM images were obtained using a fast-scanning AFM system (Nano Live Vision, RIBM, Tsukuba, Japan) with a silicon nitride cantilever (resonant frequency = 1.0−2.0 MHz, spring constant = 0.1−0.3 N/m, EBD Tip radius <15 nm, Olympus BLAC10EGS-A2). The sample (2 μL) was adsorbed on a freshly cleaved mica plate (Φ 1.5 mm, RIBM Co. Ltd., Tsukuba, Japan) for 5 min at room temperature and then washed with the same buffer solution three times. Tapping mode was employed for scanning.

Agarose Gel Electrophoresis for Analyzing Photo Responses of Hexagonal Dimers. Hexagonal monomers were first prepared and used as makers to confirm the dimer dissociating into monomers. Photoirradiation to samples was carried out by light source of Xe-lamp (300 W, Ashahi-Spectra MAX-303) at 40 °C in a water bath. The light wavelength was switched by filter (UV: 350 nm, MX0350, Φ 25 mm; Visible: 450 nm, LX0450, Φ 25 mm, Asahi Spectra Co. Ltd.) After the photoirradiation, the samples were kept in the dark at room temperature. The samples were loaded to electrophoresis on a 0.6% agarose gel containing 5 mM $MgCl_2$ in a TBE (Tris-borate-EDTA) buffer solution under 90 V at 4 °C. The gels were then imaged using ethidium bromide as staining dye by Wealtec Dolphin-View 2 (KURABO Industries, Ltd.). The intensities of bands were quantified by ImageJ software (NIH).

Spectroscopic Measurement. Fluorescence spectra were measured on JASCO FP-8300 with thermal-controlling mode. Photoirradiation to the samples was performed in a microcell placed in the cell holder of the spectrometer by keeping the temperature at 40 °C. The spectrum was directly measured after the photoirradiation. Excitation wavelength for FAM was 490 nm and fluorescence emission was recorded at 516 nm.

■ ASSOCIATED CONTENT

Ⓢ Supporting Information

Additional AFM images and DNA sequences of DNA origami scaffold. This material is available free of charge via the Internet at http://pubs.acs.org.

■ AUTHOR INFORMATION

Corresponding Author

endo@kuchem.kyoto-u.ac.jp; hs@kuchem.kyoto-u.ac.jp

Notes

The authors declare no competing financial interest.

■ ACKNOWLEDGMENTS

We thank Prof. H. Asanuma (Nagoya University) for helpful comments. This work was supported by Core Research for Evolutional Science and Technology (CREST) of JST and Grant-in-Aid for Scientific Research from MEXT, Japan. Financial support from Nagase Science and Technology

Foundation to M.E. is also acknowledged. Y.Y. was supported by China Scholarship Council (CSC).

REFERENCES

(1) Rothemund, P. W. K. *Nature* **2006**, *440*, 297−302.
(2) Rajendran, A.; Endo, M.; Sugiyama, H. *Angew. Chem., Int. Ed.* **2012**, *51*, 874−890.
(3) Saccà, B.; M. Niemeyer, C. M. *Angew. Chem., Int. Ed.* **2012**, *51*, 58−66.
(4) Endo, M.; Katsuda, Y.; Hidaka, K.; Sugiyama, H. *Angew. Chem., Int. Ed.* **2010**, *49*, 9412−9416.
(5) Nakata, E.; Fong, L. W.; Uwatoko, C.; Kiyonaka, S.; Mori, Y.; Katsuda, Y.; Endo, M.; Sugiyama, H.; Morii, T. *Angew. Chem., Int. Ed.* **2012**, *51*, 2421−2424.
(6) Saccà, B.; Meyer, M.; Erkelenz, M.; Kiko, K.; Arndt, A.; Schroederm, H.; Rabe, K. S.; Niemeyer, C. M. *Angew. Chem., Int. Ed.* **2010**, *49*, 9378−9383.
(7) Zhao, Z.; Jacovetty, E. L.; Liu, Y.; Hao, Y. *Angew. Chem., Int. Ed.* **2011**, *50*, 2041−2044.
(8) Endo, M.; Yang, Y.; Emura, T.; Hidaka, K.; Sugiyama, H. *Chem. Commun.* **2011**, *47*, 10743−10745.
(9) Kuzyk, A.; Schreiber, R.; Fan, Z.; Pardatscher, G.; Roller, E. M.; Högele, A.; Simmel, F. C.; Govorov, A. O.; Liedl, T. *Nature* **2012**, *483*, 311−314.
(10) Yoshidome, T.; Endo, M.; Kashiwazaki, G.; Hidaka, K.; Bando, T.; Sugiyama, H. *J. Am. Chem. Soc.* **2012**, *134*, 4654−4660.
(11) Yun, J. M.; Kim, K. N.; Kim, J. Y.; Shin, D. O.; Lee, W. J.; Lee, S. H.; Lieberman, M.; Kim, S. O. *Angew. Chem., Int. Ed.* **2012**, *51*, 912−915.
(12) Högberg, B.; Liedl, T.; Shih, W. M. *J. Am. Chem. Soc.* **2009**, *131*, 9154−9155.
(13) Zhang, F.; Nangreave, J.; Yan Liu, Y.; Yan, H. *Nano Lett.* **2012**, *12*, 3290−3295.
(14) Zhang, H.; Chao, J.; Pan, D.; Liu, H.; Huang, Q.; Fan, C. *Chem. Commun.* **2012**, *48*, 6405−6407.
(15) Zhao, Z.; Liu, Y.; Yan, H. *Nano Lett.* **2011**, *11*, 2997−2300.
(16) Endo, M.; Sugita, T.; Katsuda, Y.; Hidaka, K.; Sugiyama, H. *Chem.—Eur. J.* **2010**, *16*, 5362−5368.
(17) Rajendran, A.; Endo, M.; Katsuda, Y.; Hidaka, K.; Sugiyama, H. *ACS Nano* **2011**, *5*, 665−671.
(18) Endo, M.; Sugita, T.; Rajendran, A.; Katsuda, Y.; Emura, T.; Hidaka, K.; Sugiyama, H. *Chem. Commun.* **2011**, *47*, 3213−3215.
(19) Asanuma, H.; Liang, X.; Nishioka, H.; Matsunaga, D.; Liu, M.; Komiyama, M. *Nat. Protoc.* **2007**, *2*, 203−212.
(20) Liang, X.; Mochizuki, T.; Asanuma, H. *Small* **2009**, *5*, 1761−1768.
(21) Tanaka, F.; Mochizuki, T.; Liang, X.; Asanuma, H.; Tanaka, S.; Suzuki, K.; Kitamura, S.; Nishikawa, A.; Ui-tei, K.; Hagiya, M. *Nano Lett.* **2010**, *10*, 3560−3565.
(22) Endo, M.; Yang, Y.; Suzuki, Y.; Hidaka, K.; Sugiyama, H. *Angew. Chem., Int. Ed.* **2012**, *51*, 10518−10522.
(23) Castro, C. E.; Kilchherr, F.; Kim, D.-N.; Shiao, E. L.; Wauer, T.; Wortmann, P.; Bathe, M.; Dietz, H. *Nat. Methods* **2011**, *8*, 221−229.